

5,20-Diphenyl-10,15-bis(*p*-tolyl)-21-selenaporphyrin and Its Nickel(II) Complexes¹

Lechosław Latos-Grażyński,*[†] Ewa Pacholska,[†] Piotr J. Chmielewski,[†]
Marilyn M. Olmstead,[‡] and Alan L. Balch[‡]

Department of Chemistry, University of Wrocław, 50 383 Wrocław, Poland, and Department of
Chemistry, University of California, Davis, California 95616

Received March 22, 1995[©]

The synthesis of a new monoheteroporphyrin, 5,20-diphenyl-10,15-bis(*p*-tolyl)-21-selenaporphyrin (SeDPDTPH), is reported. The 21-selenaporphyrin has been characterized by ¹H NMR, ¹³C NMR, mass spectrometry, and UV–visible spectra and an X-ray structural analysis. The free base selenaporphyrin SeDPDTPH crystallizes in the monoclinic space group *P*2₁/*n* with *a* = 19.848(3) Å, *b* = 8.8410(14) Å, *c* = 20.503(4) Å, β = 103.375(12)° at 125 K with *Z* = 4. Refinement of all 4577 unique reflections and 453 parameters yielded *R*₁ = 0.096 (based on *F*²). The presence of selenium atom elongates the macrocycle along the N(1)–N(3) axis when compared to a regular porphyrin. The π delocalization pattern is altered in the selenophene moiety in relation to the free selenophene. SeDPDTPH undergoes a two-step proton addition in solution. Mono- and dication formation results in distortion of the planar 21-selenaporphyrin structure. The monocation structure is solvent dependent as shown by the ¹H NMR titration experiments. Insertion of Ni(II) into 21-selenaporphyrin yields Ni^{II}(SeDPDTP)Cl (*S* = 1, μ_{eff} = 3.3 μ_B). The electronic spectrum of this complex is porphyrin-like with a strong Soret band at 433 nm. The ¹H NMR spectra of the high-spin nickel(II) complexes of 21-selenaporphyrin have been recorded and assigned by means of the selective deuteration, line width considerations, and a 2D COSY experiment. The characteristic pattern of pyrrole (downfield) and selenophene (upfield) resonances has been established. Direct σ–π spin density transfer has been proposed to explain the upfield shift of the selenophene protons. Imidazole replaces the chloride ligand to form five- and six-coordinate complexes. The spectroscopic and chemical properties of Ni^{II}(SeDPDTP)–Cl resemble those of nickel(II) complexes with 21-thiaporphyrin. To account for these similarities, we suggest that the selenophene moiety is bent out of the porphyrin plane in Ni^{II}(SeDPDTP)Cl. Such a geometry allows metal ion to interact with selenium of selenophene in a side-on fashion.

Introduction

Replacement of the nitrogen atoms of porphyrins with other potential donors produces porphyrin related macrocycles with differing central cavity sizes. Such macrocycles may provide an interesting environment for metal ions and their chemical and the structural properties of these remain to be explored.^{2–9} Some effort has been devoted to the systematic development of macrocyclic systems where modification of porphyrin has

been achieved by introduction of other donors (O, S, Se, NCH₃, NO, N–C–, CH) to replace or modify one of the pyrrole nitrogens (Chart 1).

In this series the coordination chemistry of N-alkylated (arylated) porphyrins was extensively explored in search for the models of “green pigments”.² Limited reports on the oxaporphyrins, dithiaporphyrins, diselenoporphyrins, tetrathiaporphyrin dication, and tetraselenaporphyrin dication have appeared.^{6–10} Recently we have investigated the coordinating properties of the new member of the heteroporphyrin family, i.e. 5,10,15,20-tetra(*p*-tolyl)-2-aza-21-carba-porphyrin (inverted porphyrin).⁸ This ligand coordinates to nickel(II) with the formation of a nickel(II)–carbon bond. The synthesis and characterization of a macrocyclic ligand, 5,10,15,20-tetraphenyl-21-thiaporphyrin (STPPH), in which one of the pyrrole moieties is replaced by thiophene,⁷ offered unique possibilities to explore coordinating properties of thiophene.¹¹ Thiaporphyrin coordinates a large

* To whom correspondence should be addressed.

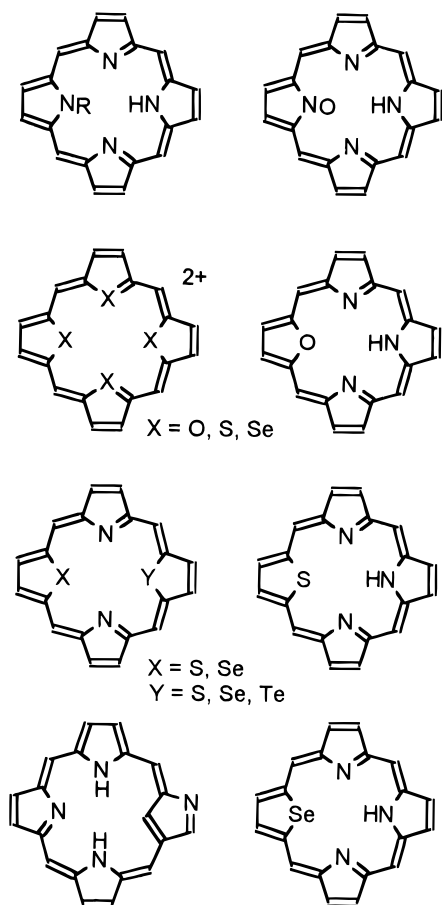
[†] University of Wrocław.

[‡] University of California.

[©] Abstract published in *Advance ACS Abstracts*, December 15, 1995.

- (1) Abbreviations: SeDPDTP, 5,20-diphenyl-10,15-bis(*p*-tolyl)-21-selenaporphyrin anion; SeDPDTPH, 5,20-diphenyl-10,15-bis(*p*-tolyl)-21-selenaporphyrin; STPP, 5,10,15,20-tetraphenyl-21-thiaporphyrin anion; STPPH, 5,10,15,20-tetraphenyl-21-thiaporphyrin; TPP, 5,10,15,20-tetraphenylporphyrin dianion; TPPH₂, 5,10,15,20-tetraphenylporphyrin; NCH₃TPP, N-methyltetraphenylporphyrin anion; NCH₃TPPH, N-methyltetraphenylporphyrin.
- (2) (a) Lavalley, D. K. *The Chemistry and Biochemistry of N-substituted Porphyrins*, VCH Publisher Inc.: New York, 1987. (b) Saito, S.; Hano, H. A. *Proc. Natl. Acad. Sci. U.S.A.* **1981**, *78*, 5508. (c) Augusto, G.; Kunze, K. L.; Ortiz de Montellano, P. R. *J. Biol. Chem.* **1982**, *257*, 6231. (d) Lanceon, D.; Cocolios, P.; Guillard, R.; Kadish, K. M. *J. Am. Chem. Soc.* **1984**, *106*, 4472. (e) Balch, A. L.; Renner, M. W. *J. Am. Chem. Soc.* **1986**, *108*, 2603. (f) Wyslouch, A.; Latos-Grażyński, L.; Grzeszczuk, M.; Drabent, K.; Bartzak, T. *J. Chem. Soc. Chem. Commun.* **1988**, 1377.
- (3) (a) Balch A. L.; Chan, Y.-W.; Olmstead, M. M.; Renner, M. W. *J. Am. Chem. Soc.* **1985**, *107*, 2393. (b) Balch, A. L.; Chan, Y.-W.; Olmstead, M. M. *J. Am. Chem. Soc.* **1985**, *107*, 6510. (c) Groves, J. T.; Watanabe, Y. *J. Am. Chem. Soc.* **1986**, *108*, 7836. (d) Tsurumaki, H.; Watanabe, Y.; Morishima, I. *J. Am. Chem. Soc.* **1994**, *115*, 11784.
- (4) (a) Callot H. J.; Chevri er, B.; Weiss, R. *J. Am. Chem. Soc.* **1978**, *100*, 1324. (b) Mansuy, D.; Morgenstern-Badrau, I.; Lange, M.; Gans, P. *Inorg. Chem.* **1982**, *21*, 1427. (c) Balch, A. L.; Cheng, R.-J.; La Mar, G. N.; Latos-Grażyński, L. *Inorg. Chem.* **1985**, *24*, 2651.
- (5) (a) Broadhurst, M. J.; Grigg, R.; Johnson, A. W. *J. Chem. Soc., C* **1971**, 3681. (b) Johnson A. W. In *Porphyrins and Metalloporphyrins*; Smith, K. M., Ed.; Elsevier: Amsterdam, 1975; p 279.
- (6) (a) Ulman, A.; Manassen, J. *J. Am. Chem. Soc.* **1975**, *97*, 6540. (b) Ulman, A.; Manassen, J.; Frolow, F.; Rabinovich, D. *Tetrahedron Lett.* **1978**, 168. (c) Ulman, A.; Manassen, J. *J. Chem. Soc., Perkin Trans. I* **1979**, 1066. (d) Ulman, A.; Manassen, J.; Frolow, F.; Rabinovich, D. *Inorg. Chem.* **1981**, *20*, 1987. (e) Abraham, R. J.; Leonard, P.; Ulman, A. *Org. Magn. Reson.* **1984**, *22*, 561.
- (7) Latos-Grażyński, L.; Lisowski, J.; Olmstead, M. M.; Balch, A. L. *J. Am. Chem. Soc.* **1987**, *109*, 4428.
- (8) Chmielewski, P. J.; Latos-Grażyński, L.; Rachlewicz, K.; Głowiak, T. *Angew. Chem., Int. Ed. Engl.* **1994**, *33*, 779.
- (9) Furuta, H.; Asano, T.; Ogawa, T. *J. Am. Chem. Soc.* **1994**, *116*, 767.
- (10) (a) Vogel, E.; Haas, W.; Krupp, B.; Lex, J.; Schmickler, H. *Angew. Chem., Int. Ed. Engl.* **1988**, *27*, 406. (b) Vogel, E.; Rohring, P.; Sicken, M.; Knipp, B.; Herrman, A. Pohl, M.; Schmickler, H.; Lex, J. *Angew. Chem., Int. Ed. Engl.* **1989**, *28*, 1651.

Chart 1



variety of metal ions to form four-, five-, and six-coordinate complexes.^{7,12-16} The thiophene fragment is bent out of the plane of the macrocycle. This bending opens up the center to accommodate the metal ion and allows it to bind the thiophene sulfur. The thiophene is η^1 -bonded to the metal through a pyramidal sulfur atom.^{13-15,18} The flexibility of the thiaporphyrin allows it to accommodate metal ions of different ionic sizes including Ni(II) and Ni(I).^{13,15} The characteristic ESR and ¹H NMR parameters of Ni(I) coordinated to thiaporphyrin have been established.¹⁹⁻²¹ Nickel(II) and nickel(I) porphyrins and related compounds have been widely studied because of the growing interest in nickel(II) hydrocorphinoid derivatives, i.e. factor F₄₃₀ which was identified as the active site of the coenzyme M methyl reductase (from *Methanobacterium thermoautotrophicum*).²² In light of the interesting properties of

nickel thiaporphyrin complexes, especially their ability to stabilize low oxidation states^{15,17,21} and to form paramagnetic organometallic complexes,²⁰ we have decided to synthesize and investigate other monoheteroporphyrin analogs.

In this paper we have begun our studies of a new macrocycle, i.e. 21-selenaporphyrin. A crucial component of this core-modified porphyrin is a selenophene ring. The coordination properties of this moiety are of substantial interest. The presence of the large selenium atom shrinks the macrocycle core size relative even to thiaporphyrin. Selenophene itself is regarded as a weakly bonding ligand that is capable of binding of metal ions in the η^1 -Se, η^2 , η^4 , η^5 or in bridging fashions.²³ As a part of our continuing program of investigation of a general relationship between the isotropic shift pattern and molecular and electronic structures of paramagnetic nickel(II) porphyrins,^{19-21,24} we now report on the synthesis and characterization of 21-selenaporphyrin and its nickel(II) complexes.

Results and Discussion

Synthesis and Spectroscopic Investigation of 21-Selenaporphyrins. 5,20-Diphenyl-10,15-bis(*p*-tolyl)-21-selenaporphyrin (SeDPDTPH) can be prepared in the reasonable yield by employing the analogous procedure as described previously for 21-thiaporphyrins.^{7,17} The synthesis is one-pot reaction from 2,5-bis(phenylhydroxymethyl)selenophene, *p*-tolylaldehyde, and pyrrole (a 1:6:7 molar ratio) in dichloromethane. The concentrations of reagents were chosen to optimize yield of the process. The synthetic route to the selenaporphyrin allows for the introduction of unsymmetrical substituents on the porphyrin periphery which have a structurally defined relationship to the location of the selenophene ring. The electronic spectra of the 21-selenaporphyrin and its protonated forms are shown in Figure 1.

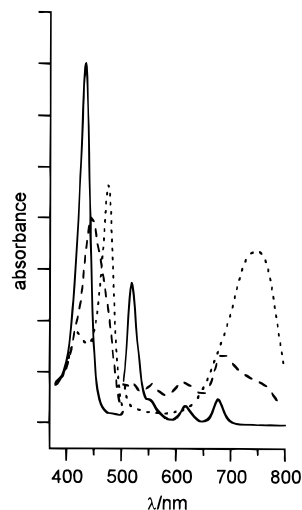


Figure 1. UV/vis absorption spectra of SeDPDTPH (solid line), SeDPDTPH₂⁺ (dashed line), and SeDPDTPH₃²⁺ (dotted line) in dichloromethane solution. The absorbance scale is arbitrary.

As usual with electronic spectra of porphyrins, there is an intense Soret band in the near-ultraviolet region and four Q

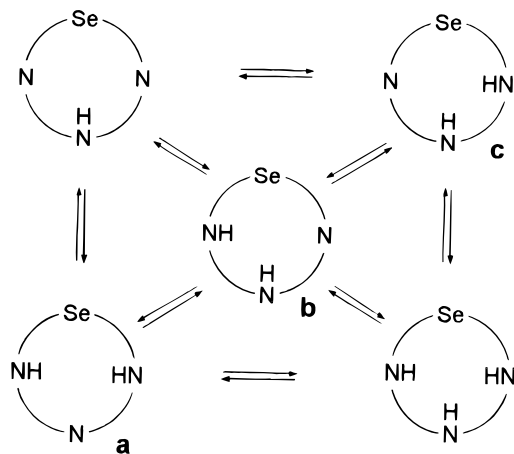
- (11) Rauchfuss, T. B. *Progress in Inorganic Chemistry*; Lippard, S. J., Ed.; John Wiley & Sons Inc.: New York, 1991; Vol. 39.
- (12) Lisowski, J.; Grzeszczuk, M.; Latos-Grażyński, L. *Inorg. Chim. Acta.* **1989**, *161*, 153.
- (13) Latos-Grażyński, L.; Lisowski, J.; Olmstead, M. M.; Balch, A. L. *Inorg. Chem.* **1989**, *28*, 1183.
- (14) Latos-Grażyński, L.; Lisowski, J.; Olmstead, M. M.; Balch, A. L. *Inorg. Chem.* **1989**, *28*, 3328.
- (15) Latos-Grażyński, L.; Olmstead, M. M.; Balch, A. L. *Inorg. Chem.* **1989**, *28*, 4065.
- (16) Pandian, R. P.; Chandrashekar, T. K. *J. Chem. Soc., Dalton Trans.* **1993**, 119.
- (17) Chmielewski, P.; Grzeszczuk, M.; Latos-Grażyński, L.; Lisowski, J. *Inorg. Chem.* **1989**, *28*, 3546.
- (18) Latos-Grażyński, L.; Lisowski, J.; Chmielewski, P. J.; Grzeszczuk, M.; Olmstead, M. M. *Inorg. Chem.* **1994**, *33*, 192.
- (19) Lisowski, J.; Latos-Grażyński, L.; Szyrenberg, L. *Inorg. Chem.* **1992**, *31*, 1933.
- (20) Chmielewski, P. J.; Latos-Grażyński, L. *Inorg. Chem.* **1992**, *31*, 5231.
- (21) Chmielewski, P. J.; Latos-Grażyński, L.; Pacholska, E. *Inorg. Chem.* **1994**, *33*, 1992.

- (22) (a) Pfaltz, A. In *The Bioinorganic Chemistry of Nickel*; Lancaster, J. R., Jr., Ed.; VCH Publishers Inc.: New York, 1988; p 275. (b) Jaun, B. In *Metal Ions in Biological Systems*; Sigel, H., Sigel, A., Eds.; Marcel Dekker, Inc.: New York, 1993; Vol. 29, p 287.
- (23) (a) Oefele, K. *Chem. Ber.* **1966**, *99*, 1732. (b) Oefele, K.; Dotzauer, E. *J. Organomet. Chem.* **1972**, *42*, C87. (c) Choi, M. G.; Angelici, R. J. *J. Am. Chem. Soc.* **1990**, *112*, 7811. (d) *J. Am. Chem. Soc.* **1991**, *113*, 5651. (e) Arce, A. J.; Deeming, A. J.; Desantctis, Y.; Machado, R.; Manzur, J.; Rivas, C. *J. Chem. Soc., Chem. Commun.* **1990**, *22*, 1568.
- (24) Latos-Grażyński L. *Inorg. Chem.* **1985** *24*, 1681.

Table 1. ^1H NMR Spectral Data for SeDPDTPH and Its Cationic Forms

	selenophene	pyrrole		
		trans δ (ppm)	cis	
			ν_1 (ppm)	ν_2 (ppm) ^e
SeDPDTPH ^a	10.03	8.88 ^c	8.66	8.61
SeDPDTPH ^b	10.06	8.92 ^d	8.67	8.62
SeDPDTPH ₂ ⁺ ^{a,f}	9.98	8.85	8.68	8.61
	9.90	8.79	8.71	8.62
SeDPDTPH ₂ ⁺ ^{b,f}	9.93	8.83	8.75	8.64
SeDPDTPH ₃ ²⁺ ^{a,g}	9.57	8.59	8.83	8.64
SeDPDTPH ₃ ²⁺ ^{b,g}	9.59	8.64	8.92	8.71

^a CDCl_3 solution, 293 K. ^b CD_2Cl_2 solution, 293 K. ^c $^4J = 2.21$ Hz. ^d $^4J = 1.94$ Hz. ^e $^3J_{\text{AB}} = 4.6$ Hz. ^f One equivalent of trifluoroacetic acid added. ^g Two equivalents of trifluoroacetic acid added.

Scheme 1

bands in the visible region. In comparison with TPPH₂, the absorption position of the Soret band for SeDPDTPH showed a large bathochromic shift. Marked bathochromic shifts of two Q bands (I and II) were also observed while bands III and IV were less affected. The electronic spectrum of SeDPDTPH resembles closely that of its thiaporphyrin analog STPPH.¹² Systematic bathochromic shifts of the Soret band and three out of four Q bands were found. The Q band showed a 9 nm hypsochromic shift. The effect is smaller than that found for tetraphenyldiselenaporphyrin.⁶

Protonation of 21-Selenaporphyrin. Spectroscopic titration of SeDPDTPH with trifluoroacetic acid in dichloromethane solution gave results similar to those obtained for STPPH.¹² The green mono- and dicationic forms were obtained. Well-defined isosbestic points were found for each protonation step. The conjugated acids of SeDPDTPH showed sizable bathochromic shifts of the Soret band. The number of Q bands is reduced due to the protonation. The protonation process was also followed by ^1H NMR spectroscopy. The ^1H NMR spectral parameters of SeDPDTPH, SeDPDTPH₂⁺, SeDPDTPH₃²⁺ are presented in Table 1.

The general protonation pattern is proposed in Scheme 1.

The ^1H NMR spectrum of SeDPDTPH unambiguously locates the NH proton on the pyrrole ring in the trans position to the selenophene moiety as indicated by the long-range coupling to the adjacent C–H group ($^4J_{\text{HH}} = 2.04$ Hz). The ^1H NMR titration in dichloromethane-*d* was carried out at 298 K. The smooth changes of the averaged shifts of the SeDPDTPH cationic forms were observed through the titration. The addition of the first proton resulted in the increase of the chemical shifts of cis pyrrole resonances. Simultaneously the selenophene and

Table 2. Selected Bond Lengths and Angles for SeDPDTPH

Bond Lengths			
Se–C(18)	1.850(7)	Se–C(1)	1.868(7)
N(1)–C(6)	1.370(9)	N(1)–C(3)	1.381(9)
N(2)–C(8)	1.380(9)	N(2)–C(11)	1.422(9)
Bond Angles (deg)			
C(18)–Se–C(1)	88.3(3)	C(6)–N(1)–C(3)	105.7(6)
C(8)–N(2)–C(11)	108.4(6)	C(2)–C(1)–Se	122.0(6)

trans pyrrole resonances were slightly moved upfield. The ^1H NMR spectra of the monocationic form reflect fast exchange between symmetric a and two asymmetric forms b and c (Scheme 1). The second protonation was accompanied by a remarkable upfield shift of selenophene and trans pyrrole resonances. The protonation behavior is different from that one established previously for thiaporphyrin in dichloromethane-*d*₂ at 298 K.¹² The titration at 203 K in dichloromethane-*d*₂ demonstrated very broad but separate resonances for the monocationic and dicationic forms. The monoprotonated form(s) gave a modest shift change for all pyrrole and selenophene resonances similar to the observation made at 298 K. The dicationic form presented the similar shifts as that established at 298 K. In addition the 22,24-NH and 23-NH resonances, not seen at the lower acid concentration or in higher temperature, were observed at -0.86 and -1.40 ppm respectively.

We have also observed that the change from dichloromethane-*d*₂ to chloroform-*d* as solvent plays an essential role in the distribution of monocationic tautomers. One could expect selective, smooth changes of the shifts of cis pyrrole resonances as seen in dichloromethane-*d*₂, accompanied by the modest changes of the selenophene and trans pyrrole resonances in the course of titration in chloroform-*d*. Unexpectedly we have established the formation of two monoprotonated species. The first one presented the separate resonances at fixed positions up to the 1:1 TFA–selenaporphyrin molar ratio, the second remained in the fast exchange with following dicationic species. We presume that the formation of the ionic pairs is responsible for the complexity of investigated equilibria. The originally formed monocation is converted into the monocation–TFA ion pair as the concentration of the required anion increased. Probably such a structural rearrangement facilitates the fast intermolecular proton exchange between mono- and dicationic forms.

The parallel titration of SeDPDTPH in chloroform-*d* resulted in a behavior similar to that observed for SeDPDTPH but clearly distinct from the one previously found for dichloromethane-*d*₂.¹²

The protonation of SeDPDTPH resulted in the characteristic shift changes due to the electric charge redistribution in the macrocycle (Table 1) that deshields protons after protonation of nitrogens. On the other hand the positive charge of the porphyrin core requires the distortion of the macrocycle from planarity. Such a rearrangement reduces the ring current effect and produces the upfield shift. The combination of these mechanisms, as described previously for thiaporphyrin,¹² accounts also for the chemical shift variation in the course of the SeDPDTPH protonation.

Structure of SeDPDTPH. The structure of SeDPDTPH was investigated by X-ray crystallography. Table 2 contains selected interatomic distances and angles.

Figure 2 shows a perspective view of the selenaporphyrin. The introduction of unsymmetrical substituents on the selenaporphyrin periphery did not entirely prevent disorder in the selenium position. In addition to the major position two sites of minor occupancy, Se(A) and Se(B), were found. These are both near N(2) and represent alternate orientation of the

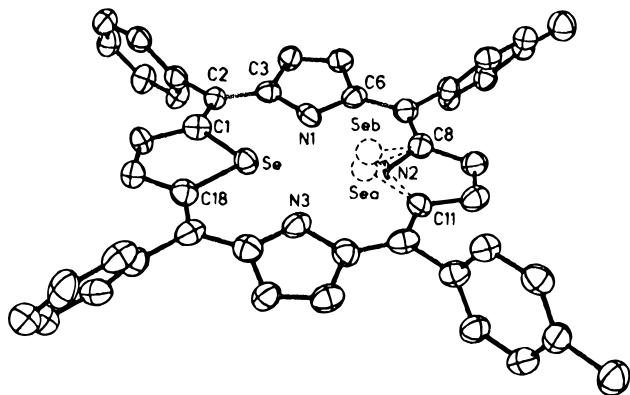


Figure 2. Perspective view of SeDPDTPH showing 50% thermal contours for all non-hydrogen atoms. The positions of the disordered selenium atoms of the minor forms are shown with dashed lines.

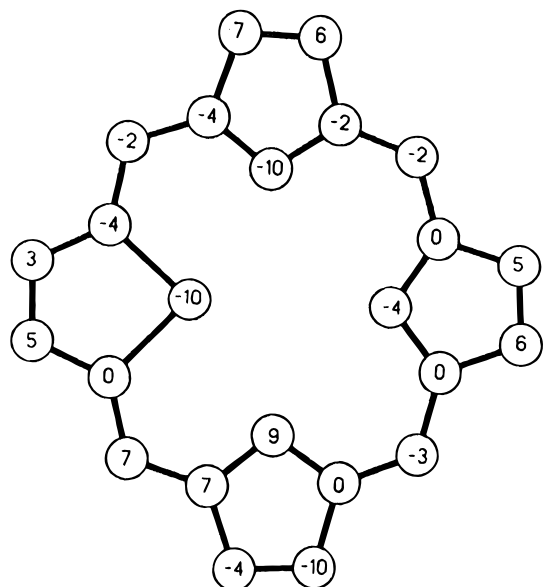


Figure 3. Formal diagram for the 21-selenaporphyrin core in which each atom symbol is replaced by a number showing the displacement (in 0.01 Å) of that atom from the mean plane of the porphyrin.

porphyrin in which the entire molecule is rotated by 180° about the N(1)–N(3) axis. Occupancies of these alternate sites are low, 3.5% at Se(A) and 1.5% at site Se(B). Related disorder was also observed for thiaporphyrins.^{7,25} The molecule is slightly distorted from planarity. This is best described by considering the out-of-plane distances from the mean plane of the porphyrin core as shown in Figure 3.

The hydrogen atom bond to nitrogen N(2), as found in the ¹H NMR experiment, was not located. Because of the presence of selenium, the core size of the macrocycle is constricted: the nonbonded Se–N(2) distance is 3.36 Å while the nonbonded N(1)–N(3) distance is 4.49 Å. Notice that Se–N(2) distance would be slightly shortened if the selenaporphyrin were strictly planar. The relevant distances in 21-thiaporphyrin and dithiaporphyrin present the similar pattern (STPP: S–N(2) 3.547–(8) Å, N(1)–N(3) 4.40(1) Å; S₂TPP: S–S 3.069(6) Å; N–N 4.65(1) Å).²⁵ A Se–Se distance of 2.85 Å was quoted from an unpublished structure of Se₂TPP (which gave no other information on the macrocycle of diselenaporphyrin).^{6b} The nonbonded N(1)–N(3) distance in SeDPDTPH is longer than in monothiaporphyrin but shorter than for dithiaporphyrin. The presence of the heteroatom elongates the macrocycle along the N(1)–

N(3) axis when compared with tetraphenylporphyrin. The corresponding N–N distances are 4.108 Å in the tetragonal form and 4.06–4.20 Å in the triclinic form of tetraphenylporphyrin.^{26,27} The Se–N distance is slightly shorter than the sum of van der Waals radii of selenium and nitrogen (3.45 Å) but longer than a typical Se–N single bond (1.824–1.845 Å).²⁸

We have found that extensive delocalization exists in the SeDPDTPH macrocycle and extends on the selenophene fragment. There is an appreciable effect of the aromatic character of the macrocycle on the selenophene portion. The Se–C_α distance remains practically unchanged in selenaporphyrin (1.850(7) Å) relative to that for free selenophene (1.855(1) Å).²⁹ The C_α–C_β distances are longer and the C_β–C_β distances are shorter in the macrocyclic structure (C_α–C_β 1.420(1) Å, C_β–C_β 1.384(10) Å) than in free selenophene (C_α–C_β 1.369(1) Å, C_β–C_β 1.433(3) Å). The C_α–Se–C_α angles are respectively equal: 87.46(4) (selenophene) and 88.3(3)° (SeDPDTPH). The pattern of C_α–C_β and C_β–C_β distances follows that seen in the pyrrole rings. These bond length changes indicate that π delocalization of the selenophene moiety is altered in 21-selenaporphyrin. Previously similar changes in the π delocalization were determined for the thiophene moiety in the mono- and dithiaporphyrins.²⁴

Formation and Characterization of a Nickel(II) Complex.

Nickel(II) can be inserted into SeDPDTPH to give a five-coordinate complex, Ni^{II}(SeDPDTP)Cl, which has good solubility in dichloromethane, chloroform, toluene, and tetrahydrofuran. Solutions of Ni^{II}(SeDPDTP)Cl are stable enough to be chromatographed, but the complex does undergo gradual demetalation in solution to give free SeDPDTPH.

The electronic absorption spectrum of Ni^{II}(SeDPDTP)Cl is presented in Figure 4.

The complex has a spectral characteristic that resembles those of metalloporphyrins. Thus the intense features at 433 and 481 nm correspond to the porphyrin Soret bands and the weaker bands in the visible region are related to the metalloporphyrin Q band absorption. Due to the lower symmetry of selenaporphyrin, the low-energy portion of the spectrum is more complex than that found for the corresponding porphyrin complexes. The electronic spectra that accompany modifications of the coordination sphere, exemplified here by imidazole coordination, are also included in Figure 4. We have noticed that the replacement of the axial ligand for the five-coordinate species produces only minor changes in the spectrum. However the coordination of two axial ligands to form the six-coordinate species could be easily observed.

Ni^{II}(SeDPDTP)Cl is paramagnetic. The magnetic moment as measured by the Evans technique in chloroform-*d* solution at 300 K is 3.3(1) μ_B. Thus complex, like Ni^{II}(STPP)Cl, has a high-spin ground state with *S* = 1.

Considering the essential similarities of the ¹H NMR spectra of Ni^{II}(SeDPDTP)Cl and Ni^{II}(SDPDTP)Cl, including the anomalously unique upfield positions of selenophene or thiophene protons (*vide infra*), we have argued that selenaporphyrin coordinates in the identical fashion as thiaporphyrins,^{7,13–15,18}

(26) Hamor, M. J.; Hamor, T. A.; Hoard, J. L. *J. Am. Chem. Soc.* **1964**, *86*, 1938.

(27) Silbers, S. J.; Tulinsky, A. *J. Am. Chem. Soc.* **1967**, *89*, 3331.

(28) Roesky, R. W.; Weber, K.-L.; Seseke, U.; Pinkert, W.; Noltemeyer, M.; Clegg, W.; Sheldrick J. *Chem. Soc., Dalton Trans.* **1985**, 565 and references cited therein.

(29) (a) Bird, C. W.; Cheeseman, G. W.; In *Comprehensive Heterocyclic Chemistry*; Katritzky, A. R., Rees, C. W., Eds.; Pergamon Press: Oxford, England, 1984; Vol. 4, pp 3–4. (b) Magdesieva, N. N. *Adv. Heterocycl. Chem.* **1970**, *12*, 1. (c) Pozdeev, N. M.; Akumlimin, O. B.; Shapkin, A. A.; Magdesieva, N. N. *Dokl. Akad. Nauk. SSSR* **1969**, *19*, 192.

(25) Latos-Grażyński, L.; Lisowski, J.; Sztrenberg, L.; Olmstead, M. M.; Balch, A. L. *J. Org. Chem.* **1991**, *56*, 4043.

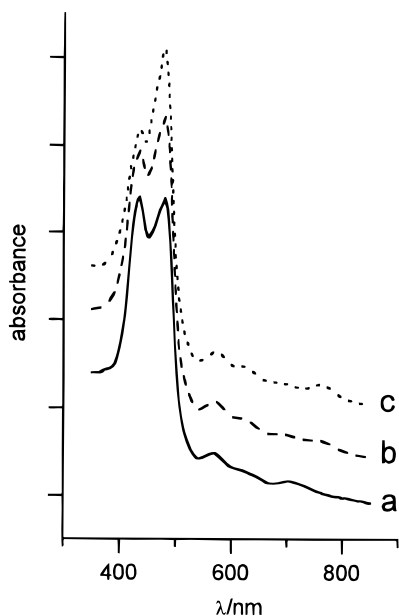


Figure 4. UV/vis absorption spectra of Ni^{II}(SeDPDTP)Cl (solid line), Ni^{II}(SeDPDTP)Cl after addition of 1 equiv of imidazole (dashed line), and Ni^{II}(SeDPDTP)Cl after addition of 30 equiv of imidazole (dotted line) in dichloromethane solution. The absorbance scale is arbitrary.

i.e., the ligand is nonplanar. Thus the selenophene moiety has to be bent out of the porphyrin plane, the metal ion interacts with selenium in a side-on fashion and the molecule appears to have effective C_s symmetry in solution with the mirror plane passing through the nickel atom, the axial chloride ligand, and the selenophene selenium.

The ¹H NMR spectrum of Ni^{II}(SeDPDTP)Cl is shown in Figure 5. The ¹H NMR data have been analyzed in the context of the effective C_s geometry. In this case there are three distinct pyrrole protons' positions and one selenophene position. Two ortho and meta positions on each phenyl ring will be distinguishable because of the perpendicular orientation of these rings with respect to the porphyrin plane and the restricted rotation about *meso*-carbon-to-phenyl bond.³⁰ The resonance assignments which are given above each peak have been made on basis of relative intensities, line width analysis, and the ¹H NMR 2D COSY experiment. The most characteristic feature, the upfield peak at -38.9 ppm (298 K), corresponds to the selenophene protons. There are three, downfield-shifted pyrrole resonances. The ¹H 2D COSY experiment revealed the coupling between resonances of the cis pyrrole ring (Figure 5, trace b). The remaining pyrrole resonance corresponds to the trans pyrrole. Resonances in trace c of Figure 5 come from phenyl protons. They fall into two groups according to their line width. Four broader resonances are assigned to ortho protons, since these should relax more efficiently because they are close to the paramagnetic Ni(II) ion.³⁰ The remaining resonances have been assigned to the meta protons of 5,20-phenyl and 10,15-*p*-tolyl rings. The *p*-CH₃ resonance could be easily identified at 4.0 ppm. A two-dimensional COSY experiment was carried out to connect protons within the phenyl (*p*-tolyl) groups. Cross-peaks reveal pairwise coupling between ortho and meta protons within the *p*-tolyl and phenyl rings. Two further cross-peaks revealed the connectivity of meta and para protons of the 5,20 phenyls.

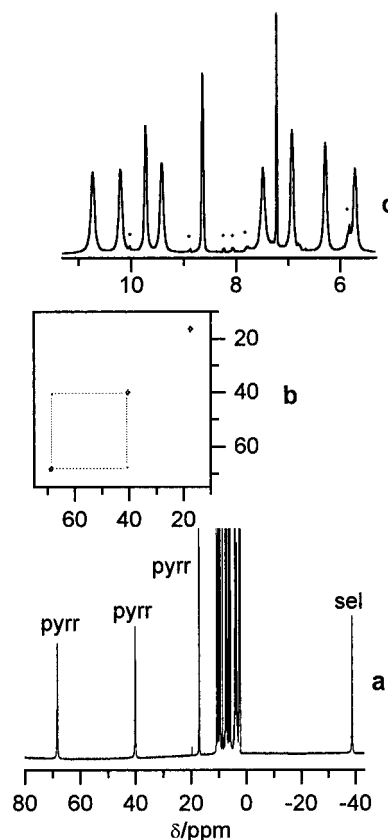


Figure 5. (a) 300 MHz ¹H NMR spectra of Ni^{II}(SeDPDTP)Cl in CDCl₃. Resonances of the pyrrole protons are labeled pyrr; selenophene protons, sel. (b) Selected part of ¹H 2D COSY plot. A cross-peak connecting resonances of 7-H and 8-H pyrrole resonances is shown. (c) Expansion of phenyl resonances.

Table 3. Chemical Shifts of Nickel(II) Selenaporphyrin Complexes

	selenophene	pyrrole	
		cis	trans
Ni ^{II} (SeDTDPP)Cl ^a	-38.7	68.3	40.2
[Ni ^{II} (SeDTDPP)Im]Cl ^b	-33.5	66.5	35.9
[Ni ^{II} (SeDTDPP)Im ₂]Cl ^c	-35.7	68.7	36.0
[Ni ^{II} (SeDTDPP)(CD ₃ OD) ₂]Cl ^d	-35.1	68.6	37.1

	thiophene	pyrrole	
		cis	trans
Ni ^{II} (STPP)Cl ^a	-24.0	55.4	29.7

^a CDCl₃ solution, 293 K. ^b CDCl₃ solution, 293 K, 1 equiv of imidazole added. ^c CDCl₃ solution, 293 K, 30 equiv of imidazole added. ^d CD₃OD solution, 298 K.

In this experiment we have identified the cross-peak only for the adjacent protons (ortho–meta, meta–para). In the phenyl ring the spin-spin coupling varies ($^3J \gg ^4J$) and the correlations due to the small couplings, i.e. for more distant protons, are expected to be very weak.³¹ The results of this assignment were used to identify the resonances of the individual *meso*-substituents and are presented in Tables 3 and 4 and in Figure 6. Since each ortho proton presented single cross-peaks to the adjacent meta proton, they could be used as the starting point in the further analysis.

The two ortho and two meta protons on each ring are inequivalent since the porphyrin plane bears different substituents on opposite sides of the macrocycle. The Ni^{II}(SeDPDTP)-

(30) (a) La Mar, G. N.; Walker, F. A. In *Porphyrins*; Dolphin, D., Ed.; Academic Press: New York, 1979; Vol. IVB, p 61. (b) Bertini, I.; Luchinat, C. In *NMR of Paramagnetic Molecules in Biological Systems*; The Benjamin/Cumming Publishing Co. Inc.: Menlo Park, CA, 1986.

(31) Keating, K. A.; de Ropp, J. S.; La Mar, G. N.; Balch, A. L.; Shiao, F.-Y.; Smith, K. M. *Inorg. Chem.* **1991**, *30*, 3258.

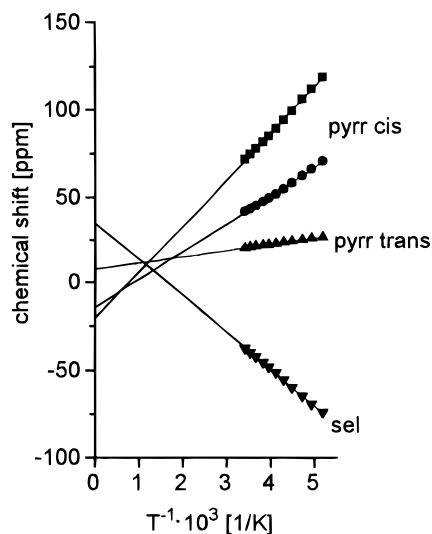


Figure 6. Curie plots of the chemical shifts of the pyrrole and selenophene resonances of $\text{Ni}^{\text{II}}(\text{SeDPDTP})\text{Cl}$.

Table 4. Chemical Shifts [ppm] for Meso Substituents of $\text{Ni}^{\text{II}}\text{SeDPDTPCl}$ (in CDCl_3)

	phenyl	tolyl
ortho	8.66	10.76
	6.94	6.30
meta	10.23	9.75
	9.44	8.66
para	5.72	4.0 (<i>p</i> - CH_3)

Cl spectrum corresponds to the situation where the rotation is relatively slow (298 K, CDCl_3 , 300 MHz) rendering ortho and meta protons inequivalent.

The effects of temperature on the ^1H NMR spectrum of $\text{Ni}^{\text{II}}(\text{SeDPDTP})\text{Cl}$ are shown in Figure 6 where the chemical shifts of pyrrole and selenophene resonances are plotted versus $1/T$. The chemical shifts show linear behavior with extrapolated intercepts that do not correspond to the corresponding diamagnetic reference. This behavior can be ascribed to the temperature dependent contributions of two different delocalization pathways (*vide infra*). The markedly different spectrum of $\text{Ni}^{\text{II}}(\text{SeDPDTP})\text{Cl}$ in methanol- d_4 (Table 3) is attributed to displacement of the axial chloride and the formation of $[\text{Ni}^{\text{II}}(\text{SeDPDTP})(\text{CD}_3\text{OD})_2]\text{Cl}$.

Imidazole Coordination. The addition of imidazole and N-methylimidazole has been followed by ^1H NMR. Titration of a 2 mM solution of $\text{Ni}^{\text{II}}(\text{SeDPDTP})\text{Cl}$ with imidazole in CDCl_3 shows the gradual growth of a new set of resonances while the resonances of the starting material diminish in intensity. The spectrum of the product is shown in trace a of Figure 7.

All resonances of the coordinated imidazole are clearly discernible. Their integrated intensities indicate that only one imidazole ligand is bound in the first step of the reaction. Identical spectra have been obtained when $\text{Ni}^{\text{II}}(\text{SeDPDTP})\text{ClO}_4$ (prepared directly in the NMR tube by an addition of AgClO_4) was used. This observation, along with the fact that overall pattern of the selenophene resonances and relative line widths appear to be retained in the spectrum of the imidazole adducts, indicates that imidazole replaces the axial anion to form $[\text{Ni}^{\text{II}}(\text{SeDPDTP})(\text{Im})]\text{Cl}$. The imidazole resonances have been identified through suitable deuteration(s). The ^1H NMR data are summarized in Tables 3 and 5.

The spectra obtained for imidazole-2-*d* and imidazole-3-*d* are shown in traces b and c of Figure 7. The resonance of the 2-H is readily assigned since it is missing in the spectrum of $[\text{Ni}^{\text{II}}(\text{SeDPDTP})(\text{Im})]\text{Cl}$.

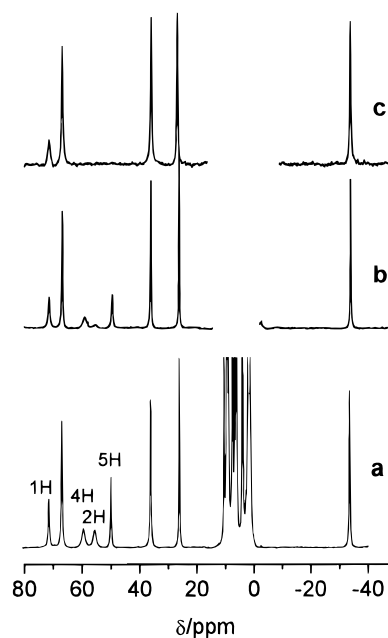


Figure 7. 300 MHz ^1H NMR spectra of 2 mM chloroform-*d* solutions of $\text{Ni}^{\text{II}}(\text{SeDPDTP})\text{Cl}$ in the presence of (a) imidazole, (b) imidazole-2-*d*, and (c) imidazole-*d*₃ (1:1 molar ratio, 293 K).

Table 5. Chemical and Isotropic Shifts of Coordinated Imidazole

	chem shift ^a	isotropic shift ^b
NH	71.0	58.3
2-H	55.3	54.3
4-H	59.2	58.7
5-H	49.6	45.2

^a CDCl_3 solution, 298 K, 1 equiv of imidazole added. ^b Diamagnetic standards of coordinated imidazole as in ref 37.

$(\text{SeDPDTP})(\text{imidazole-2-}d)\text{Cl}$. All but the 1-NH imidazole resonance are missing in the spectrum of the imidazole-*d*₃ adduct. The 4-H resonance is assigned on the basis of its line width (360 Hz) which is similar to that of the 2-H resonance (370 Hz). Both are expected to be at similar distances from the nickel(II) ion and both should have comparable line widths that are greater than those of the other imidazole resonances (NH 150 Hz, 5-H 120 Hz). At ratios of imidazole to $\text{Ni}^{\text{II}}(\text{SeDPDTP})\text{Cl}$ higher than 1.1:1, the coordinated imidazole resonances have not been detected because of exchange broadening. Smooth changes of the chemical shifts of the pyrrole and selenophene resonances have been observed in the further course of the titration. Under these conditions the six-coordinated compound $[\text{Ni}^{\text{II}}(\text{SeDPDTP})(\text{Im})_2]\text{Cl}$ is in rapid exchange with the five-coordinate form. The formation of the six-coordinate species resulted mainly in an additional 14.1 ppm downfield shift of the trans pyrrole resonance. The asymptotic shift values of the six-coordinate complex, represented here by $[\text{Ni}^{\text{II}}(\text{SeDPDTP})(\text{CH}_3\text{OD})_2]$ (Table 3), were not attained even with a 30:1 molar ratio (Table 3). The resonance assignment of selenaporphyrin resonances for the five-coordinate $[\text{Ni}^{\text{II}}(\text{SeDPDTP})(\text{Im})]^+$ follows those for $\text{Ni}^{\text{II}}(\text{SeDPDTP})\text{Cl}$. Relatively small changes of shifts due to coordination of one nitrogen base have been measured for selenophene and cis pyrrole resonances. The largest change in the downfield direction was seen for the trans pyrrole resonance. The resonance assignments for $[\text{Ni}^{\text{II}}(\text{SeDPDTP})(\text{Im})_2]\text{Cl}$ have based upon correlation with the resonances of $\text{Ni}^{\text{II}}(\text{SeDPDTP})\text{Cl}$ in the course of the titration. The titration of $\text{Ni}^{\text{II}}(\text{SeDPDTP})\text{Cl}$ with 1-methylimidazole exhibits similar behavior through the complete concentration range. However, the axial ligand lability precludes observation of the resonances of the coordinated ligand.

Analysis of Hyperfine Shift. It is generally argued that the dipolar contribution to isotropic shift is negligible for five- or six-coordinate Ni(II) compounds.³² Sizable dipolar shifts can arise as a result of the anisotropy of the zero field splitting. The dipolar shift arising from ZFS has a characteristic T^{-2} dependence for high-spin d^8 electronic structure which is in contrast to the T^{-1} dependence expected for contact shifts.^{32,33} However, the opposite direction of deviations from Curie behavior (Figure 6), seen for pyrrole and selenophene resonances, excludes the dipolar term as the major reason for such behavior. On the other hand, the directions of the phenyl shifts in $Ni^{II}(\text{SeDPDTP})\text{Cl}$ are compatible with a dominant π -contact contribution and a small dipolar contribution. The dipolar mechanism in $Ni^{II}(\text{NCH}_3\text{TPP})\text{Cl}$ also contributed less than 10% to the pyrrole shifts.²⁴ The downfield shift of pyrrole resonances is indicative of σ -delocalization of spin density and is consistent with the ground state of Ni(II) which has two unpaired electrons in the σ -symmetry orbitals ($(d_{x^2-y^2})^1(d_{z^2})^1$).

A large difference in the contact shifts of the pyrrole resonances is seen even for protons located on the same pyrrole ring. The spread of shifts is related to the Ni(II) coordination number (Table 3). The upfield shift of the selenophene resonance requires special comment. The suggested side-on-coordination of the selenophene moiety changes the pathways of the spin delocalization in this ring. This tilting should reduce the σ -effect for the selenophene hydrogens, since the mechanism is strongly dependent on geometry.¹⁹ The unpaired spin density is localized on the selenium σ orbital that is not orthogonal to the π -orbitals of the selenaporphyrin, and σ - π overlap within the selenophene ring will permit the direct transfer of unpaired spin density from the selenium σ pair into the π system(s) without any π ligand-Ni(II) bonding. The spread of pyrrole resonances results from delocalization of positive π spin density (upfield shift). Previously we described the π delocalization of unpaired spin density in nickel(II) thiaporphyrin in terms of ligand-to-metal and metal-to-ligand charge transfer.¹⁹ Spin densities at the particular carbons were related to the pattern of the occupied π and unoccupied π^* molecular orbitals. The patterns of thiaporphyrin π molecular orbitals were calculated using the semiquantitative Fenske-Hall LCAO MO method.^{19,34} The direct involvement of the singly occupied $d_{x^2-y^2}$ orbital of Ni(II) and σ orbitals of sulfur included into the extensive conjugation of the folded thiaporphyrin was required. The extent of mixing of thiaporphyrin molecular orbital with $d_{x^2-y^2}$ of nickel was ascertained by considering first the symmetry, and then the overlap between Ni(II) and thiaporphyrin orbitals.¹⁹ Here we assume that similar pathways are operating for selenaporphyrin and that the molecular orbitals of selenaporphyrin resemble those of thiaporphyrin. The similarity of ^1H NMR and electronic spectra of seleno- and thiaporphyrin and their nickel(II) complexes support such a thesis.

The strong similarities in pyrrole, selenophene and phenyl paramagnetic shift patterns in the halide and mono R-imidazole complexes allow us to conclude that the shift origins are predominantly contact in both cases. The shifts for the various imidazole protons as listed in Table 5 are downfield for the NH, 2-H, 4-H, and 5-H protons. This pattern is generally consistent with major contribution from σ -spin delocalization³⁵⁻³⁷

as described previously for $[Ni^{II}(\text{SDPDTP})(\text{R-Im})]\text{Cl}$.¹⁹ and other nickel(II)-imidazole complexes.³⁸⁻⁴¹

Conclusions

5,20-Diphenyl-10,15-bis(*p*-tolyl)-21-selenaporphyrin and its nickel(II) complexes have been synthesized and characterized. The geometry of SeDPDTPH as shown by an X-ray structure is slightly distorted from planarity with the major out-of-plane distortion caused by need to accommodate large selenium atom in the porphyrin crevice. It is apparent the new macrocyclic analog of the porphyrin, modified at coordinating core, can coordinate nickel(II) ion to form five- and six-coordinate complexes. It requires the strong distortion of the macrocycle to accommodate the selenophene ring and the postulated η^1 -bonding of pyramidal selenium. ^1H NMR studies indicated that the replacement of the sulfur of SDPDTPH by selenium to produce SeDPDPH perturbs in a rather small extent the electronic structure of the macrocycle and its nickel(II) complexes. Our studies provide the first example of the Se-bound selenophene complex of a first row transition metal. The coordination chemistry of selenaporphyrin appears to be similar to that of thiaporphyrin.^{7,8,11-21,23}

Experimental Section

Solvents and Reagents. Chloroform-*d* (Glaser), dichloromethane (CIL), and methanol-*d*₄ (IBJ) were used as received.

Substituted imidazoles (all from Aldrich), and imidazole (Im), were purified by standard procedures. Imidazole-2-*d* (Im-2-*d*) and imidazole-*d*₄ (Im-*d*₄) were prepared according to reported methods.⁴² Imidazole-*d*₄ was used as a source of imidazole-*d*₃ since the ND is easily replaced by the residual water in solution to form NH. Silver perchlorate (Aldrich) was recrystallized from acetonitrile and dried in very small portions directly before use.

Preparation of Compounds. SeDPDTPH. 2,5-Bis(phenylhydroxymethyl)selenophene was synthesized as previously described.^{6,43} 2,5-Bis(phenylhydroxymethyl)selenophene, 1 g (3 mmol), with *p*-tolylaldehyde, 2.15 mL (18 mmol), and pyrrole, 1.4 mL (21 mmol), were added to deoxygenated dichloromethane (500 mL). After addition of boron trifluoride etherate (4 mmol) the reaction mixture was stirred in the dark. *p*-Chloranil, 5.9 g (24 mmol) (Fluka), was added and the solution was refluxed (1 h) and then taken to dryness under reduced pressure by rotatory evaporation. The product was dissolved in dichloromethane and chromatographed on a neutral alumina column to remove tarry products. Chromatography on silica gel (Mesh 270) was carried out. The SeDPDTPH fraction (brown-orange) was eluted with benzene/cyclohexane (3:1 v/v), evaporated to dryness, and recrystallized from methanol/dichloromethane (1:1 v/v) to produce 250 mg of selenaporphyrin, yield: 12%.

Anal. Calcd for $\text{C}_{46}\text{N}_3\text{H}_{33}\text{Se}$: C, 78.18; H, 4.71; N, 5.95; Found: C, 78.10; H, 4.76; N, 5.97.

UV/vis (λ , nm (log ϵ): 433 (5.11), 518 (4.30), 552 (3.56), 618 (3.46), 667 (3.62).

(32) La Mar, G. N., Horrocks, W. D., Holm, R. H., Eds. *NMR of Paramagnetic Molecules* Academic Press: New York, 1974; Chapters 1 and 4.

(33) (a) Kurland R. J.; Mc Garvey, B. R. *J. Magn. Reson.* **1970**, *2*, 286. (b) Bleaney, B. J. *J. Magn. Reson.* **1972**, *8*, 91.

(34) Hall, M. B.; Fenske, R. F. *Inorg. Chem.* **1972**, *11*, 768.

(35) Wicholas, M.; Mustatch, R.; Johnson, B.; Smedley, T.; May, J. J. *Am. Chem. Soc.* **1975**, *97*, 2113.

(36) Balch, A. L.; Chan, Y.-W.; La Mar, G. N.; Latos-Grażyński, L.; Renner, M. W. *Inorg. Chem.* **1985**, *24*, 1437.

(37) Satterlee, J. D.; La Mar, G. N. *J. Am. Chem. Soc.* **1976**, *98*, 2804.

(38) Wu, F.-J.; Kurtz, D. M., Jr. *J. Am. Chem. Soc.* **1989**, *111*, 6563.

(39) Tovrog, B. S.; Drago, R. S. *J. Am. Chem. Soc.* **1974**, *96*, 2804.

(40) Claramunt, R.-M.; Elquero, J.; Jacquier, R. *Org. Magn. Reson.* **1971**, *3*, 595.

(41) Tovrog, B. S.; Drago, R. S. *J. Am. Chem. Soc.* **1977**, *99*, 2203.

(42) Vaugh, J. D.; Mugharbi, Z.; Wu, E. C. *J. Org. Chem.* **1970**, *31*, 1141.

(43) Eglinton, G.; McCrae, W. *Adv. Org. Chem.* **1963**, *4*, 225.

^{13}C NMR (75.47 MHz, CDCl_3): δ 136.1 (2,3-C, selenophene); 136.0, 132.2 (cis pyrrole-C); 128.7 (trans pyrrole-C); 134.4, 132.2 (C-ortho); 127.8, 127.4 (C-meta), 127.6 (C-para), 21.6 (*p*- CH_3). Carbon resonance assignments were obtained via a ^{13}C - ^1H correlated experiment.

Mass spectrum (EI): calcd $m/z = 707$; found m/z 707.

$\text{Ni}^{\text{II}}(\text{SeDPDTP})\text{Cl}$. A solution of 100 mg (0.7 mmol) of NiCl_2 in 5 mL of methanol was added to a solution of 50 mg (0.07 mmol) of 5,20-diphenyl-10,15-bis(*p*-tolyl)-21-selenaporphyrin in 40 mL of chloroform. The solution was heated under reflux for 8 h. It was cooled, and the solvent was removed under reduced pressure. The solid residue was extracted with chloroform, and the chloroform was separated from the remaining solid by filtration. The chloroform solution was subjected to chromatography on a silica gel column (Mesh 270). Elution with chloroform gave an orange-brown fraction containing SeDPDTPH. Further elution with chloroform/methanol (100:2 v/v) produced a green fraction that was recovered as a solid after evaporation under vacuum. The solid was again dissolved in dichloromethane/methanol, filtered and the solvent was removed. It produced 10 mg of $(\text{SeDPDTP})\text{Ni}^{\text{II}}\text{Cl}$, yield 17%.

Anal. Calcd for $\text{C}_{46}\text{N}_3\text{H}_{32}\text{SeNiClCH}_2\text{Cl}_2\text{CH}_3\text{OH}$: C, 62.88; H, 4.18; N, 4.58; Found: C, 62.81; H, 4.09; N, 4.67.

The presence of the solvents has been confirmed independently by ^1H NMR.

Electronic spectrum (chloroform solution), λ nm (log ϵ): 433 (5.41), 481 (5.26), 519 (sh), 565 (4.15), 610 (sh), 677 (3.08), 704 (3.04).

Mass spectrum ($m + 1$)/ z (LSIMS): calcd 803; found 803. Spectra match the calculated isotope distribution.

Instrumentation. ^1H NMR spectra were measured on a Bruker AMX spectrometer that operated in a quadrature detection mode. Usually 1000 scans were taken. The signal to noise ratio was improved by apodization of the free induction decay which induced typically 5–15 Hz broadening. The residual ^1H NMR spectra of the deuterated solvents were used as a secondary reference. The 2D COSY spectrum of $\text{Ni}^{\text{II}}(\text{SeDPDTP})\text{Cl}$ was obtained after collecting a standard 1D reference spectrum. The 2D spectrum was collected by use of 1024 points in t_2 over the desired bandwidth (to include all desired peaks) with 256 t_1 blocks and 1024 scans per block. All experiments included four dummy scans prior to the collection of the first block.

Magnetic moment measurements were carried out by the Evans method with CDCl_3 solutions using TMS as a reference.⁴⁴ Diamagnetic corrections were obtained using the published values of the constitutive corrections for TPPH_2 ⁴⁵ and Pascal's constants. Absorption electronic spectra were recorded on a Specord M-42 spectrophotometer.

Mass spectra were recorded on a ADM-604 spectrometer using electron impact and liquid matrix secondary ion mass spectrometry and a primary beam of 8 keV Cs^+ ions.

X-ray Structure Determination. Crystals of SeDPDTPH were prepared by diffusion of methanol into the dichloromethane solution contained in a thin tube. The crystals were dark blue

Table 6. Crystallographic Data for SeDPDTPH.

empirical formula	$\text{C}_{46}\text{H}_{33}\text{N}_3\text{Se}$
color, habit	dark blue prisms
fw	706.71
cryst syst	monoclinic
space group	$\text{P}2_1/\text{n}$
a , Å	19.848 (3)
b , Å	8.8410 (14)
c , Å	20.503 (4)
β , deg	103.375(12)
V , Å ³	3500.1(10)
T , K	125(2)
Z	4
cryst size, mm	$0.14 \times 0.12 \times 0.06$
d_{calcd} , g/cm ⁻³	1.341
radiation λ , Å	1.541 78
$\mu(\text{Cu K}\alpha)$, mm ⁻¹	1.734
range of transm factors	0.81–0.91
$R_1^{a,c}$	0.0982
$wR2^{b,c}$	0.2148
R_1^d	0.0725

^a $R_1 = \sum ||F_o - F_c| / \sum |F_o|$. ^b $R_w = [\sum [w(F_o^2 - F_c^2)^2] / \sum [w(F_o^2)^2]]^{1/2}$.
^c All data. ^d Data with $F_o > 4\sigma(F_o)$.

prisms. Data were collected at 125 K on a Siemens P4/RA diffractometer that was equipped with Siemens LT-2 low temperature apparatus. Two check reflections showed random (less than 2%) variation during the data collection. The data were corrected for Lorentz and polarization effects. Crystal data are compiled in Table 6. Calculations were performed on a DEC MicroVAX 3200 with programs of SHELXL-93. Scattering factors for neutral atoms and corrections for anomalous dispersion were taken from the standard source.⁴⁶ An absorption correction was applied to the structure.⁴⁷ The solution was obtained by direct methods. A small amount of disorder in the position of the selenium adversely affected the thermal parameter of 3N(2) and prevented the location of the hydrogen atom of the porphyrin core. The disorder was treated by examining several different models which place the selenium in the nitrogen site of the pyrrole group involving N(2). The last cycles of refinement include Se(A) at 3.5% occupancy and Se(B) at 1.5% occupancy. The positional parameters of these atoms were fixed and their isotropic thermal parameters allowed to vary.

Acknowledgment. Financial support from the State Committee for Scientific Research KBN of Poland (Grant 2.0732 91 01) and the National Science Foundation (U.S.–Poland Cooperative Science Program Grant INT-9114389) is gratefully acknowledged.

Supporting Information Available: Tables giving crystal data and details of the structure determination, atomic coordinates and equivalent isotropic displacement parameters, anisotropic thermal parameters, and calculated hydrogen coordinates for SeDPDTPH and an ORTEP diagram with more complete numbering (10 pages). Ordering information is given on any current masthead page.

IC950329Z

- (46) International Tables for X-ray Crystallography; Kynoch Press: Birmingham, England, 1974; Vol. 4, p 47.
 (47) Program XABS2 calculates 24 coefficients from a least-squares fit of A^{-1} and $\sin^2(\theta)$ to a cubic equation in $\sin^2(\theta)$ by minimalization of F_o^2 and F_c^2 differences. Parkin, A., Ph.D. Thesis, University of California, Davis, 1993.

(44) Evans, D. F.; James, T. A. *J. Chem. Soc.* **1979**, 723.

(45) Eaton, S. S.; Eaton, G. A. *Inorg. Chem.* **1980**, *19*, 1095.